Contents lists available at ScienceDirect

Estuarine, Coastal and Shelf Science

Physical characteristics and discharges of suspended particulate matter at the continent-ocean interface in an estuary located in a semiarid region in northeastern Brazil

Francisco Jose da Silva Dias [a, *], Belmiro Mendes Castro [b], Luiz Drude Lacerda [c], Luiz Brunner Miranda [b], Rozane Valente Marins [c]

[a] Laboratório de Hidrodinâmica Costeira, Estuarina e de Águas Interiores (LHiCEAI), Departamento de Oceanografia e Limnologia (DEOLI), Universidade Federal do Maranhão (UFMA), São Luis, Maranhão, Brazil
[b] Laboratório de Hidrodinâmica Costeira (LHiCO), Instituto Oceanográfico (IO), Universidade de São Paulo (USP), São Paulo, SP, Brazil
[c] Laboratório de Biogeoquímica Costeira (LBC), Instituto de Ciências do Mar (LABOMAR), Universidade federal do Ceará (UFC), Fortaleza, Ceará, Brazil

ARTICLE INFO

ABSTRACT

This study reports the hydrodynamics of the transport of suspended particulate matter (SPM) in the Jaguaribe River estuary, which receives the runoff from the largest drainage basin in the state of Ceará, Brazil. The estuary is located in the semiarid region of Brazil, where rainfall occurs primarily between January and May and results in water flow rates exceeding 3000 m^{3}s^{-1}. The drainage basin contains more than 4000 dams, which, during the dry season, block most of the flow of freshwater and sediment. The net balance and transport of sediments were calculated for the wet and dry seasons considering a tidal cycle of 13 h at the interfaces between the upper and middle estuary and between the middle and lower estuary. The Jaguaribe River estuary is classified as partially mixed with weak vertical stratification and a tendency toward being well mixed. The SPM transported during the rainy season originates in the drainage basin due to high river inflow, whereas during the dry season, resuspension and hydraulic fills generated by tides causes the accumulation of SPM in the middle estuary, forming a zone of maximum turbidity. The transport of salt in the estuary was predominantly caused by gravity flow and tidal propagation.

1. Introduction

The understanding of physical processes that regulate transport from the continent to estuaries and from there to the inner continental shelf (ICS) are based on direct measurements performed in these environments. Certain classic studies (Officer, 1976; Dyer, 1986, 1987; Miranda et al., 2002) highlight the complexity of studying the hydraulics of suspended fine sediments (cohesive and non-cohesive) and those transported by saltation due to the intrinsic hydrodynamic characteristics of estuarine systems. The deficit or accumulation of sediments in coastal zones can significantly alter the development of the coastline and result in losses and gains in coastal areas and damage to civilian structures (French et al., 2008; Valle-Levinson, 2010; Syvitski and Kettner, 2011).

Increased loads of suspended particulate matter due to watershed development (Syvitski et al., 2005; Milliman and Farnsworth, 2011) cause considerable impacts on estuarine and marine ecosystems. These impacts include sedimentation (Weber et al., 2012; Flores et al., 2012), elevated turbidity reducing photic depth (Fabricius et al., 2013, 2014), and stressors associated with pollutants attached to sediment such as nutrients and trace metals (Dias et al., 2013a,b; Weber et al., 2006).

Delandmeter et al. (2015) showed that sediments are deposited and retained in a bay near a river mouth, while suspended sediments that travel longer distances are transported within freshwater plumes during flood events. Thus, at the continent-ocean interface, the transport of suspended particulate matter becomes complex and hardly predictable in estuaries where the influence of the tide leads to an increased residence time of freshwater, and therefore of fine sediments (clays, silts), in a turbidity maximum zone (TMZ) (Dyer, 1986). As a result, the fluxes of riverine suspended particulate matter (SPM) exported to the ocean in such

* Corresponding author.
E-mail address: geofranzedias@gmail.com (F.J.S. Dias).

estuaries are currently poorly documented, due to a lack of appropriate measurements that take into account the seasonal cycles of river discharges (Fettweis et al., 1998). When available, field measurements are expensive and are either specific to a time period or a geographical location (i.e. not representative of the riverine or estuarine section); they are recorded several (sometimes hundreds of) kilometers upstream from the river mouth and do not take into account the trapping of sediments in estuaries (Ludwig et al., 1996; Schlunz and Schneider, 2000).

The Jaguaribe River is the most important river in the state of Ceará (Northeastern, Brazil); its watershed measures approximately 76,000 km^2, which is almost 50% of the state's area. Campos et al. (2000) observed that until the 1950s, the flows in the Jaguaribe River were very irregular and ranged from 0 m^{3}s^{-1} in the dry season to 7000 m^{3}s^{-1} in the rainy season. This variability led to the construction of dams as a strategy to mitigate the effects of a lack of rain during 9 months of the year and to increase water availability to meet growing urban and agricultural demands (Marins et al., 2011; IBGE, 2014).

Dams change the downstream hydrologic regime and control the flow variability, making these flows independent of rain and making the physical and chemical quality of the estuarine water dependent on a balance between low stream flows and tidal forces, which can cause erosions of ancient sedimentary deposits (Marins et al., 2003; Godoy and Lacerda, 2013), due to decreasing of freshwater discharges. High salinity has been observed as far as 30 km inland from the river mouth (30 g kg^{-1}), whereas salinity in the middle estuary may be higher than in the adjacent coastal water (34.5—36 g kg^{-1}) (Dias et al., 2013a,b). Studies conducted between 2004 and 2006 indicated that during flood tides, water velocities reached 0.58 ms^{-1} with flow rates of 350 m^{3}s^{-1}, whereas during ebb tides, velocities did not exceed 0.4 ms^{-1} with flow rates of less than 200 m^{3}s^{-1}, highlighting the effect of the decrease in stream flow on the estuary system (Dias et al., 2009). In contrast with reservoirs built for energy generation with their steady outflows and smaller downstream impacts, reservoirs for water storage such as those in the Jaguaribe River basin affect freshwater flows in estuaries only in exceptionally rainy years (Dias et al., 2011). Lacerda et al. (2012) compared the effect of dams on the Jaguaribe River estuary during the dry season after a strong rainy year with water freezing in the mouths of rivers draining into the Arctic, when river flows are blocked and the residence time (RT) in marginal lakes are longer. Whereas during the period of higher river discharge, river flows are greater and reach the adjacent coastal zone, and RTs are shorter in estuaries. The trend of increasingly short intermittent rainy seasons has resulted in a greater influence of tidal waves in the Jaguaribe River estuary and in increased colonization by mangroves (Maia et al., 2006; Godoy and Lacerda, 2015), increased water salinity (Marins et al., 2003; Dias et al., 2013a,b), enlargement of beaches, development of islands in the middle estuary, and extensive erosion at the river mouth (Godoy and Lacerda, 2013). Due to changes in estuarine dynamics, the authors have observed an impacted sedimentary system comprising the full range of particle size (from mud to sand). Therefore, a better understanding of the suspended particulate matter on the estuary and on the variations in flows and currents associated with the dry and rainy seasons is essential to understanding the mixing process and to identifying the factors that cause mixing and advective transport of salt and other chemicals. The aim of this study was to physical characterization of an estuary located in the northeast of Brazil, in the semi-arid climate, showing how the material transport, net balance and the residence time may show a high variability between the rainy season and dry, linked to hydrodynamics imposed by successive dams along the river Jaguaribe.

2. Study area

The local climate is characterized by strong seasonality and two well-defined periods: a rainy season spanning from December to May, which can last until mid-July, with the highest rainfall (positive water balance) in April, and a dry season (drought, negative water balance) spanning from June to November, with the lowest rainfall in September. The seasonality of the rainfall is controlled by the Intertropical Convergence Zone (ITCZ), which, during the austral summer, causes northeasterly trade winds to bring air masses to and produce rain in northeastern Brazil between January and May. During the second half of the year, the ITCZ is weak and associated with southeasterly trade winds, which generate the dry season (Funceme, 2010).

The highest water levels in the drainage network of the Jaguaribe River basin (Fig. 1A) historically occurred from February to April, which coincides with the period of high rainfall in the region (Godoy and Lacerda, 2013). An analysis of historic water flows in the Jaguaribe basin (ANA, 2006) indicates that the flow rates decreased from 1978 to 1989. Maximum flow rates of 2250 m^{3}s^{-1} occurred in 1985. The flow rates were significantly lower between 1990 and 2006 with an average of 24.5 m^{3}s^{-1} and peaks as high as 251.3 m^{3}s^{-1} in 1996, with a decrease of up to 10-fold in the flows rates from the Jaguaribe River basin to the estuary system. The changes in flows in the Jaguaribe River during the 20-year period of 1987—2007 reflect the increase in the number of dams in the basin and the changes in rainfall due to global climate change (Moncunil, 2006). The construction of the dams began in the mid-twentieth century and ceased in the early nineties.

The dams located along the Jaguaribe River are for increasing water availability once there is a growing demand for water. In addition to increasing the stored liquid volume, the suspended sediments are retained by dams, affecting the morphodynamic balance in the estuarine region. During the rainy season, when the rainfall is within the historic averages, the effect of the dams is despised, and the volume of freshwater and suspended sediments arrive in the estuarine region, whereas during the dry season the estuarine system behaves as a sea arm (Dias et al., 2011).

Several studies conducted in the region, Dias et al. (2009, 2011, 2013a) have shown that there is a small spatial fluctuation between the interfaces higher/middle estuary and the middle/lower estuary, and that these interfaces are located in the cities of Aracati and Fortim. The interface Higher/Middle estuary (HE/ME) shows the fluvial and materials contributions of the drainage basin to the estuarine system, whereas the interface Middle/Lower estuary (ME/LE) shows the estuarine system contribution to the inner continental shelf, according to the classification of Dias et al. (2013a,b).

Dias (2007) reported that the total water flows in the estuary between 2005 and 2006 were dominated by flood flows in September 2005 and February 2006, when a dissipative effect of the tidal wave occurred in the flood plains of the river. In June 2006, this author observed a predominance of ebb flows. At that time, the total water volume varied depending on the type of tide, and the volume of fresh water in the system reached 95% of the total volume in February 2006. During the dry season, the total water volume was 44% more than that observed in February 2006, and this phenomenon is related to the spring tide observed in September. However, the fresh water fraction varied between 11.7% and 14.7% in September 2005 and June 2006, respectively. The flushing time spanned 2 h during the dry season and 12 h during the rainy season.

Dias et al. (2013) observed the formation of an estuarine plume during a period of intense rain in 2009. This plume extended 6 km along the shoreline and occupied the upper 2 m of the water column. Based on thermohaline indices, the authors characterized
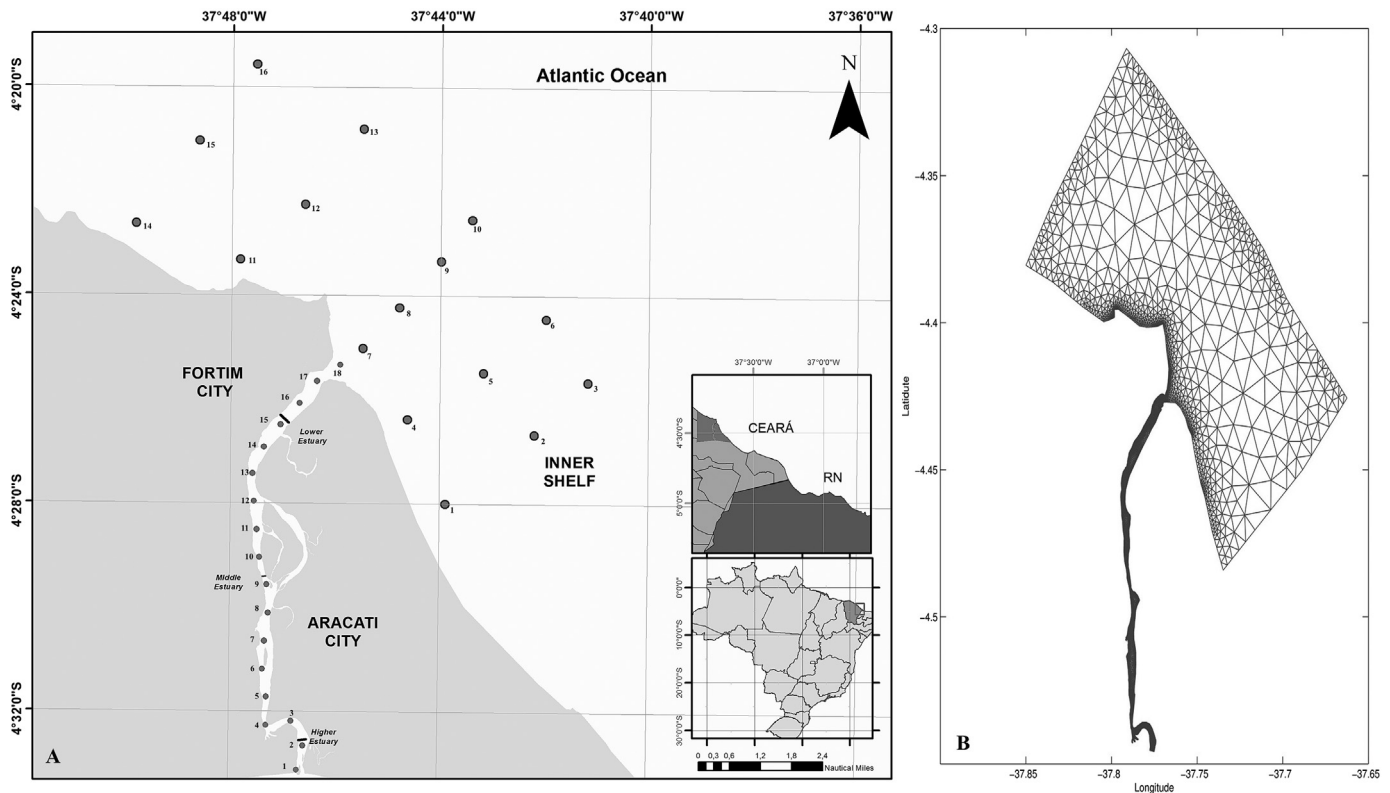
Fig. 1. A - Location map of the Jaguaribe River estuary, northeastern Brazil. Cross sections denoted by black lines are the locations of the ADCP profiles developed in May and October 2009. B - Areas represented by each SPM sampling station, i.e., Voronoi polygons, in the Jaguaribe River estuary and the Inner Continental Shelf.

three water masses: river water (RW) with temperatures higher than 29 °C and salinity of less than 30 g kg^{-1}, coastal water (CW) with temperatures between 28 °C and 29 °C and salinity between 34.5 and 36 g kg^{-1}, and tropical water (TW) with temperatures between 25 °C and 27 °C and salinity exceeding 36 g kg^{-1}.

Lacerda et al. (2013) showed that the extreme dry and rainy seasons that occurred in 2009, when total season rainfall varied from 330 mm to 8 mm between the rainy and the dry season respectively, encompassed all possibilities of flux magnitude which occurred between 2005 and 2009. During the rainy season, a positive net flux to the ocean occurred. However, even during the extreme rainy period of 2009, marine waters contributed significantly to the total flow, mostly from the estuary to the sea, as observed by much larger flows at this interface, compared to the river to estuary interface. During the dry season, discharge to the ocean was mostly due to tidal waters entering the estuary, with a small contribution from the higher basin.

Between 2005 and 2009, as a result of differences in the water flow, the water residence time in the middle estuary varied significantly between seasons. Shorter residence times of less than one day were typical of the rainy periods, when freshwater fluxes were maximal and mostly positive, as in 2009. During the rainy seasons, the proportion of fresh water to the total volume present in the estuary varied from 70% in low precipitation rainy seasons to 95% in the extreme rainy season of 2009, resulting in water residence times in the estuary that varied from 0.5 days in high-rainfall rainy seasons to a maximum of 3 days in low-rainfall rainy seasons (average 0.8 days for the rainy seasons between 2005 and 2009). In contrast, the water residence times during the dry seasons were much longer, varying from 0.2 to 13 days (average 3.1 days for the entire monitoring period) (Lacerda et al., 2013).

3. Materials and methods

Two field investigations were performed in the rainy and dry seasons at the HE/ME interface to quantify the fluvial contribution of the drainage basin to the estuary and at the ME/LE interface to quantify the contribution of the estuary to the ICS (Fig. 1). Estuarine zones were defined by Dias et al. (2009, 2011) following the methodology proposed by Miranda et al. (2002). Water properties (temperature, salinity and density) were measured at two points (left and right margins, with a distance of 120 m) at these interfaces hourly for 13 h in the wet and dry seasons. The measurements were recorded using a CTD with a rated temperature range of −5 °C to 40 °C, conductivity range of 0–90 ms cm^{-1}, and pressure range of 0–2000 dbar. The frequency of data acquisition by the CTD was 15 Hz, and the descent rate of the device was 0.5 ms^{-1}. The CTD was used as a standalone unit, and the data were stored in the device's memory. After the CTD was pulled from the water, the data were downloaded and subjected to an initial quality control procedure. Inconsistent data due to systematic and random errors were deleted, and these data gaps were filled using linear interpolation such that only the profiles with a level of interpolation of ≤5% were included in the analysis. Only the data obtained during the descent of the CTD were used because the ascent of the device involves more turbulence than the descent and disturbs the stratification of the water column.

To measure the instantaneous velocity each hour, a towed ADCP (Sontek/YSI) with a frequency of 1500 MHz was used in the direction perpendicular to the flow. Burst interval data were acquired every 5 s using 0.25-m cells at depths between 6 and 7 m in the rainy season and depths between 3 and 4 m in the dry season.

3.1. Thermohaline structure

During pre-processing of the CTD data, spurious data were detected and excluded based on a maximum rate of change of each variable; values exceeding this limit were excluded. We used a Gaussian filter to fill the gaps left by the removal of inconsistent data. After the pre-processing, we evaluated the profiles at 0.5-m depth intervals from the surface to the bottom, and values that differed from the average by more than 3 times the standard deviation of each block were eliminated (Emery and Thomson (2001).

Due to the varying height of the water column during a complete tidal cycle in the rainy and dry seasons (9.0 and 4.0 m, respectively), the sampling depth (z) was normalized by its dimensionless value (Kjerfve, 1975);

$$Z = \frac{z}{h(t)}, \tag{1}$$

where h(t) is the water depth during sampling and Z is the normalized depth. The water properties (S, T) were interpolated in the water column at intervals of 0.1 Z. The main characteristics of the time variations and the scalar properties were described on the surface (Z = 0) and near the bottom (Z = 1.0) in a regime of ebb and flood tides (Miranda et al., 2002; Bergamo et al., 2002).

After determining the values in each interval and removing the spurious values, the gaps in the temperature and conductivity data in each 0.5-m interval were filled using a moving window and a filtering procedure; the replacement values were weighted averages of adjacent values. The Gaussian window was the Hanning type. The number of adjacent values included in the average corresponded to the size of the window, and the distribution of the weightings in relation to the central value was determined by the type of window (Emery and Thomson (2001).

3.2. Currents

Profiles perpendicular to the average direction of flow were delineated, and the currents were measured during a full tide cycle (13 h) at the HE/ME and ME/LE interfaces. The vertical velocity was used as a diagnostic parameter to validate the data related to the water flow in the estuary system. Decomposition of the velocity vector relative to the local reference plane of orthogonal Cartesian coordinates Oxy was performed in the longitudinal component u (along channel) and in the transverse component v (cross channel). Following the decomposition of the velocity vector recorded each hour, the components were determined for each ith depth at each point.

The averages in space and time were numerically integrated in accordance with the methods of Miranda et al. (2002) and Bergamo et al. (2002). The vertical profiles of the scalar properties were generically denoted by P = P (Zj,t) sampled at discrete dimensionless depths (Zj = 0, −0.1, −0.2, … −1), and the averages of these profiles in time were calculated by numerical integration:

$$P(Z_j, t) > P(Z_j) = \frac{1}{T} \int_0^T P(Z_j, t) dt \tag{2}$$

Once the average profile was obtained for each dimensionless depth, the average value of the property in the water column was obtained numerically:

$$< \overline{P(Z_j, t)} > = \overline{P} = \int_{-1}^0 P(Z_j) dZ \tag{3}$$

where the symbols <> and the bar (−) indicate averages in time

and space, respectively, during intervals of time equal to a period of a complete tidal cycle (T) along the water column.

To estimate the barotropic effect of the tide, the average value of the scalar property P = P (Z,t) in the water column was calculated by numerical integration:

$$\overline{P(Z_j, t)} = \overline{P(t)} = \int_{-1}^0 P(Z, t) dZ \tag{4}$$

This value was subtracted from the corresponding quasi-stationary value of P obtained in equation (3). To calculate the average values in the areas A = A (x,Z) of the cross sections in the time interval (T) of the scalar properties P = P (A,t) = P (x,Z,t), we used the equations

$$<P(x, Z, t) \geq P(x, Z) = \frac{1}{T} \int_0^T P(x, Z, t) dt \tag{5}$$

and

$$\overline{<P(x, Z, t)>} = \overline{P} = \frac{1}{A} \iint_A P(x, Z) dx dz \tag{6}$$

When expressing average values in the water column, the property P (x,Z,t) was the longitudinal component of velocity v = v (x,Z,t), and the difference between the average value in the water column and the stationary value vt = v (x, Z, t) − < v (x, Z, t) > represented the effect of the barotropic component of the pressure gradient force.

3.3. Transport volume and residence time

The transport volume (TV) or estuarine flow in the sections perpendicular to the average flow in area A = A (x, Z) was calculated by numerical integration using the equation

$$T_V = \frac{1}{T} \int_0^T \left[\frac{1}{A} \iint_A \vec{v} \cdot \vec{N} dA \right] dt, \tag{7}$$

where $\vec{v} = \vec{v}(x, Z, t)$ is the velocity vector, $\vec{N}$ is the versor normal to section A, T is the period of a complete tidal cycle, x is the horizontal distance of the section, and Z is the depth.

To calculate the size of the tidal prism, we used the model of Officer (1976), in which TP is defined as the volume of water in the estuary between ebb and flood tide. After the variation in transport volume (TV) during a tidal cycle was calculated, the integration of transport during the time interval (Δt) corresponding to a half cycle of a semidiurnal tide is equal to the tidal prism (TP), which was calculated using the equation

$$P_M = \int_0^{\Delta t} T_V dt. \tag{8}$$

The average salinity in the estuarine system was calculated assuming a mixture of seawater (Vp) and continental water (Qf) during a semidiurnal tidal cycle and assuming that the entire volume was removed from the system at low tide. Therefore, for conservation of the mass fields (volume), we used the equation

$$S = \frac{V_P}{\left(V_P + Q_{f.}\right)} S, \tag{9}$$

where S is the average salinity in the estuary during flood and ebb tides assuming a well-mixed estuary, and S0 is the undiluted average salinity of seawater in the adjacent ocean region.

Additional details of this method were presented by Luketina (1998) and Miranda et al. (2002).

In the mixture zone (MZ), it is common to observe the effect of the longitudinal salinity gradient, indicating that because of the dilution of seawater, a portion of fresh water is retained in the estuarine system (Miranda et al., 2002). Assuming that the estuary water is the result of mixing of seawater and freshwater, the amount of freshwater (V_{fw}) was calculated using the equation

$$V_{fw} = \frac{Q_f.}{P_M} \tag{10}$$

The flushing time (T_D) and residence time (RT) represent the time that a water particle or molecule (organic or inorganic) remains in the estuarine system during flood and ebb tides. According to Ketchum (1950), the T_D of a liquid volume and the RT of organic and inorganic compounds transported and retained in the estuary system represent the ratio between the volume of freshwater (V_{fw}) retained in the MZ and the river discharge (Q_f):

$$RT = \frac{V_{fw}}{Q_f.} \tag{11}$$

3.4. Vertical instability and advective transport of salt and SPM

Vertical instability of the water column was evaluated after calculating the Richardson numbers for the estuary (Ri_e) and its layers (Ri_L). Ri_e establishes the ratio between the gain in potential energy due to river discharge and the kinetic energy of the tide and was adapted from Dyer (1974), Hunkins (1981), and Miranda et al. (2005):

$$Ri_e = \frac{g\Delta\rho_H h u_a}{\rho u_{rmq}^3}, \tag{12}$$

where $\Delta\rho_H$ is the density difference between the seawater and river water; hu_a is the river discharge per unit of width; and u_{rmq}^3 is the mean square root of the velocity generated by the barotropic effect of the tide approximated by $u_{rmq} = (\overline{u}(t) - u_a)$, where $\overline{u}(t)$ is the average velocity in the water column. The Richardson numbers of the layers (Ri_L) were calculated using the equation

$$Ri_L = \frac{gh\Delta\rho_v}{\rho u^2} \approx \frac{gh\beta\Delta S_v}{u^2}, \tag{13}$$

where h = h(t) is the local depth, $\Delta\rho_v$ and ΔS_v represent the difference between the surface and bottom density, u^2 is the average velocity in the water column, and β is the saline contraction coefficient. Values of $Ri_L \leq 2.0$ indicate vertical instability of the water column, and values of $Ri_L \geq 20.0$ indicate high vertical stability. Intermediate values of $2 < Ri_L < 20$ indicate weak vertical stability.

The average salt transport (ST) during a complete tidal cycle is divided into the components due to river discharge, Stokes derivation, tidal propagation, gravity flow, residual diffusion, tidal shear, and non-stationary effects of the wind.

$$T_s = \frac{1}{T}\int_0^T [\rho\, u\, S\, dz\,]dt = <\overline{\rho u S h}> \tag{14}$$

To determine the spatial gradient of the SPM, water samples were collected in duplicate at 18 stations along the estuary channel of the Jaguaribe River. In the ICS, samples were collected from 16 stations arranged in 5 sections perpendicular to the average direction of the 10-m isobath. SPM flows were calculated using the equation

$$T_{MPS} = \iint_A \varphi\, \vec{v}\cdot\vec{n}\, dA = \iint_A \varphi.u dA = \overline{\varphi u}A \tag{15}$$

where T_{SPM} is the discharge of SPM [kg^{-1}], u is the integrated average velocity in the water column (ms^{-1}), φ is the average concentration of SPM ($mg.L^{-1}$), and A is the average area perpendicular to the longitudinal direction of flow (m^2). The area represented by each SPM sample was delineated based on a spatialization of the area of operation of each sample using Voronoi polygons (Fig. 1B) (Aurenhammer and Klein, 1989).

4. Results and discussion

4.1. Thermohaline structure

At the HE/ME interface, the temperature during the sampling period (13 h) ranged between 29.6 °C and 30.2 °C with an average of 29.9 ± 0.2 °C (Fig. 2A). At the ME/LE interface, the pattern was similar, i.e., a range between 29.3 °C and 30.3 °C and an average of 29.9 ± 0.3 °C (Fig. 2B). The temperature ranges observed at the HE/ME and ME/LE interfaces were 0.6 °C and 1 °C, respectively, representing increases of 0.05 h^{-1} and 0.08 h^{-1}, respectively. The vertical salinity structure was essentially constant across the estuary (Fig. 2C and D) and ranged between 0.143 and 0.144 g kg^{-1} with an average of 0.142 g kg^{-1} at the HE/ME interface (Fig. 2C) and between 0.149 and 0.194 g kg^{-1} with an average of 0.171 g kg^{-1} at the ME/LE interface (Fig. 2D). The small variations in the vertical thermal and saline gradients, i.e., essentially vertical lines, indicate the homogeneity of the water column across the estuary in the rainy season due to the influence of river water, which is warmer and less saline. The high rainfall in the region during the sampling period caused high river discharges to the estuary, which are evident in the small or almost nonexistent thermal and saline gradients at the HE/ME and ME/LE interfaces.

In the dry season, the temperature at the HE/ME interface (Fig. 2E) was typical of continental water during the ebb tide and ranged between 28.9 °C and 29.5 °C, whereas during the flood tide, we observed a mixture of continental and coastal waters with a range of 28.1 °C–28.5 °C. This pattern was also observed at the ME/LE interface (Fig. 2F). The salinity of the Jaguaribe River at the HE/ME interface (Fig. 2G) displayed a pattern typical of estuarine waters and ranged between 2 and 5 g kg^{-1} during the ebb tide and between 8 and 17 g kg^{-1} during the flood tide, indicating a dilution of continental water by coastal water. The vertical orientations of the isohalines suggest complete mixing in the estuary. During the ebb tide at the ME/LE interface (Fig. 2H), we observed a typically estuarine water mass, whereas during the flood tide, there was a predominance of coastal water; the highest salinities were observed near the bottom, suggesting only slightly the presence of a salt wedge.

4.2. Current field and outflows

The current velocities in the Jaguaribe River estuary were determined at the HE/ME and ME/LE interfaces in the rainy and dry seasons of 2009. We adopt the convention u > 0 to express longitudinal velocities at ebb tides and u < 0 to express longitudinal velocities at flood tides.

In the rainy season, in the 13 profiles (Fig. 3A), the longitudinal component of the current (u) at the HE/ME interface was uniform in that all currents were discharges (u > 0) and the highest velocities were observed at the surface. At this interface, velocities reached 1.3 ms^{-1}, with an average of 0.76 ± 0.33 ms^{-1}. The same pattern was observed at the ME/LE interface (Fig. 3B): higher velocities of
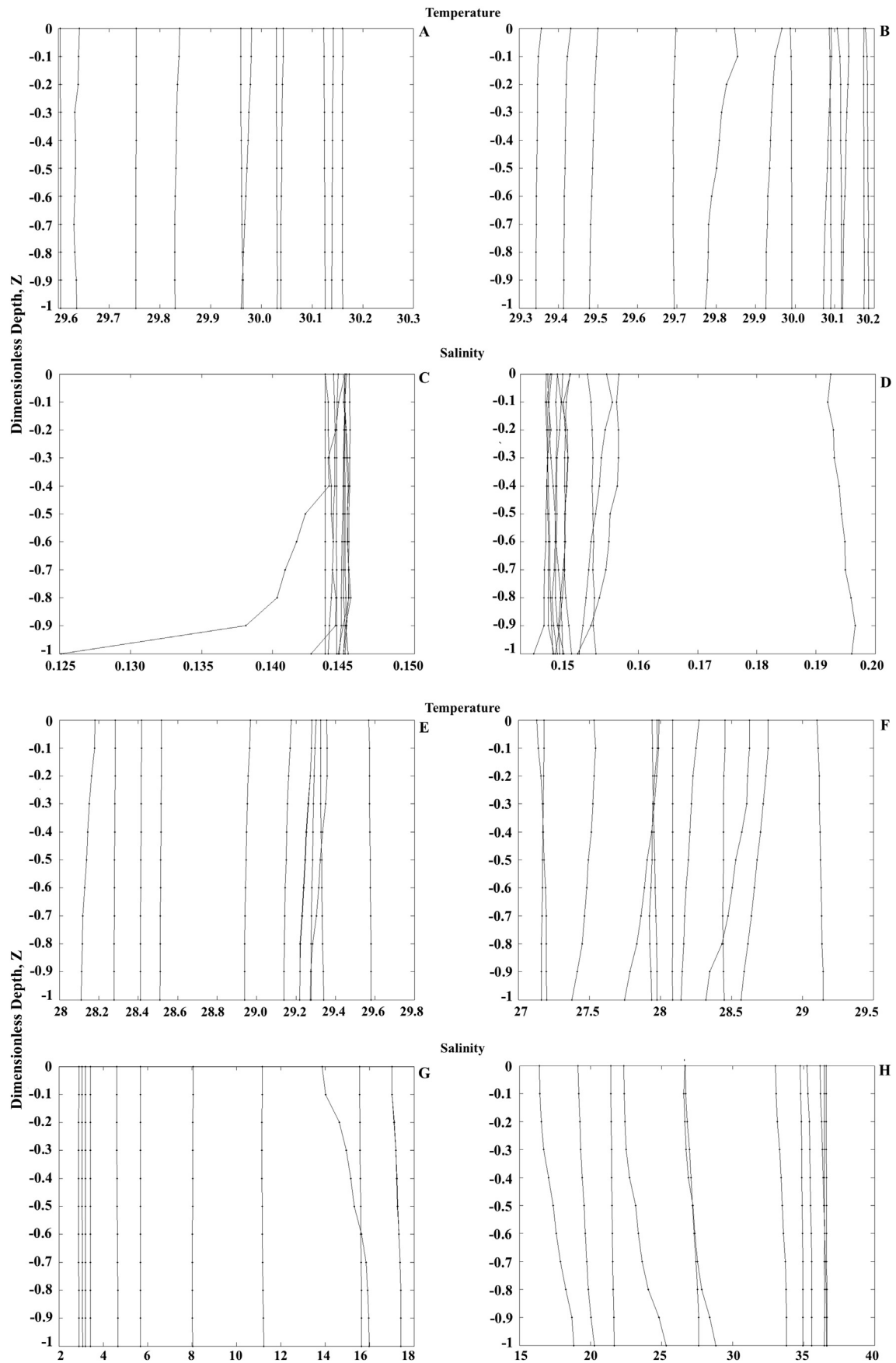
Fig. 2. Vertical variations in temperature (°C) at the HE/ME interface (A,E) and ME/LE interface (B,F) and in salinity (g.kg^{-1}) at the HE/ME interface (C,G) and ME/LE interface (D,H) in the rainy and dry seasons of 2009.
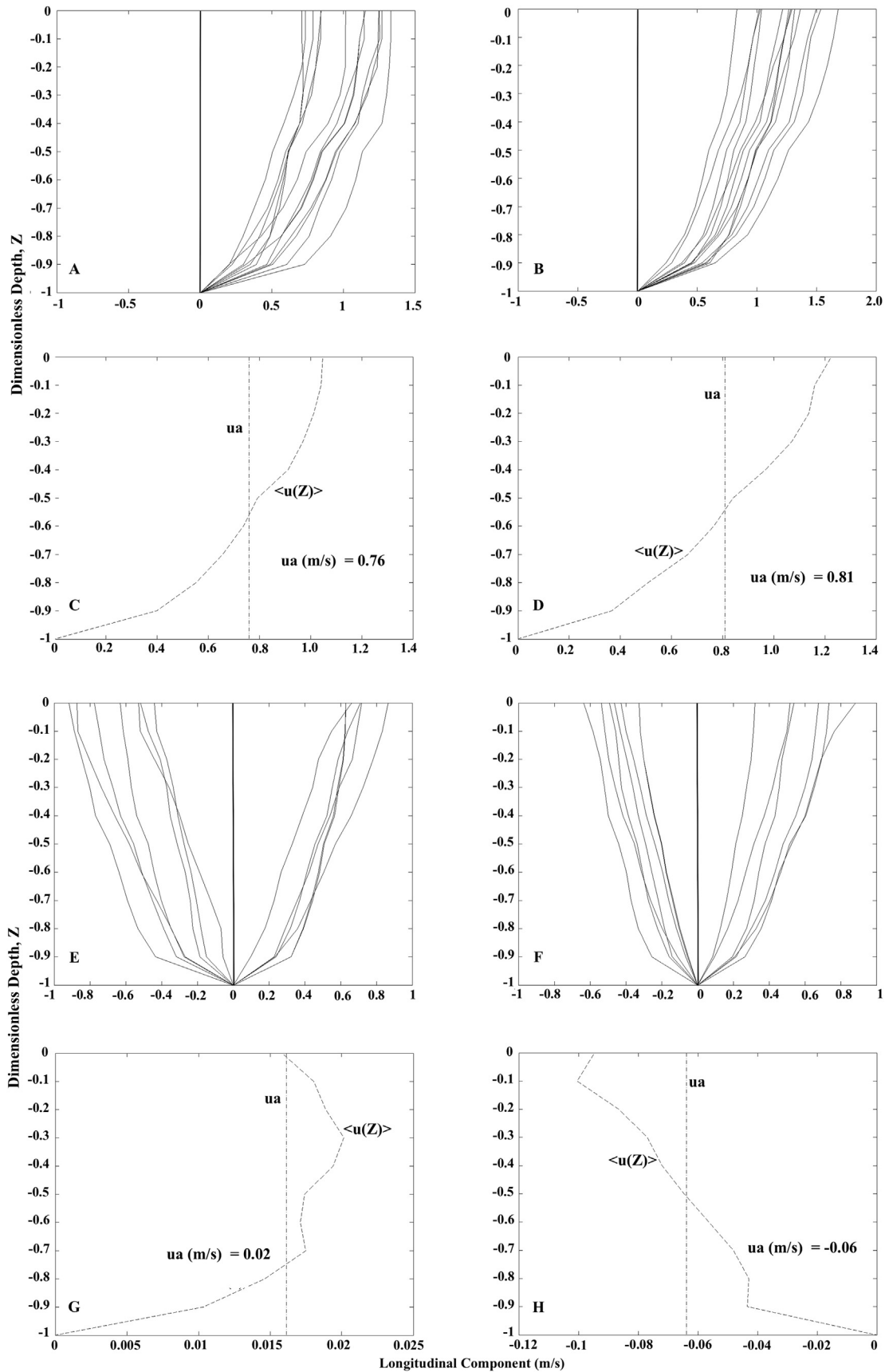
Fig. 3. Longitudinal velocities during a tidal cycle at the HE/ME(A,E) and ME/LE (B,F) interfaces and mean profiles of stationary velocity during a tidal cycle at the HE/ME(C,G) and ME/LE (D,H) interfaces in the rainy and dry seasons of 2009. u_a is the average stationary value of the longitudinal component of velocity; $\langle u(Z) \rangle$ is the average temporal profile at the dimensionless depth.

approximately 1.63 ms^{-1} at the surface and an average of 0.86 $\pm$ 0.39 ms^{-1}. A comparison of the transverse (v) and longitudinal (u) components indicates that the mean transverse component was 4-fold lower at the HE/ME interface (0.15 ms^{-1}) and at least 2-fold lower at the ME/LE interface (0.48 ms^{-1}). This greater magnitude of the longitudinal component indicates its importance to the renewal of water in the estuary system, even at times of high river discharge. The unidirectional pattern observed at both interfaces resulted from high river flows during the rainy season. The effect of the river on the estuary system is easily identified based on the gravity flow calculated from the stationary velocities, (u$_a$) (Fig. 3C and D), which were 0.76 ms^{-1} and 0.81 ms^{-1} at the HE/ME and ME/LE interfaces, respectively. The positive values of u$_a$ measured in the rainy season indicate the downstream transport in the estuary and indicate that the system was a water exporter during the period of unidirectional flow, corroborating the results obtained by Dias et al. (2011, 2013a,b).

However, in the dry season, the unidirectional flow observed in the rainy season became bidirectional at the HE/ME (Fig. 3E) and ME/LE (Fig. 3F) interfaces, demonstrating the stronger influence of tides in the system. The longitudinal velocity measured during the ebb tide (u > 0) at the HE/ME interface (Fig. 3E) ranged between 0.09 and 0.87 ms^{-1} with an average of 0.43 $\pm$ 0.23 ms^{-1}. During the flood tide (u < 0), the longitudinal velocity ranged between −0.05 and −0.91 ms^{-1} with an average of −0.42 $\pm$ 0.24 ms^{-1}. At the ME/LE interface (Fig. 3F), the longitudinal velocities ranged between 0.08 and 0.88 ms^{-1} during the ebb tide, with an average of 0.36 $\pm$ 0.22 ms^{-1}, and between −0.04 and 0.64 ms^{-1} during the flood tide, with an average of 0.27 $\pm$ 0.17 ms^{-1}.

Similar to what was observed in the rainy season, the transverse component compared with the longitudinal component during the flood tide in the dry season was an average of 2-fold lower (0.12 ms^{-1}) at the ME/LE interface and 10-fold lower (0.04 ms^{-1}) at the HE/ME interface. At low tides, the velocity of the transverse component was 4-fold lower (0.09 and 0.10 m s^{-1} at the HE/ME and ME/LE interfaces, respectively) than the longitudinal component. The bi-directionality of flow in the dry season shown in Fig. 6 demonstrates the loss of importance of the fluvial component after a period of high runoff at both interfaces, indicating that the marine component is an important agent in the renewal of estuarine water during this time of year. The pattern observed in the Jaguaribe River estuary in the dry season (Fig. 3G and H) indicates the greater influence of tides at the two interfaces. However, the stationary profile at the HE/ME interface (Fig. 6G) presented a velocity of 0.02 ms^{-1}, indicating that this interface was a location of export of water to the estuarine system. In addition, the average velocity of the stationary profile at the ME/LE interface (Fig. 6H) was −0.06 ms^{-1}, indicating that this interface was a location of import of water to the estuary.

The gravity flow downstream of the estuary in the dry season at the HE/ME interface and upstream of the estuary at the ME/LE interface suggests that the water volumes per unit area that enter the estuary system during flood tides are similar to those that leave the estuary at low tides, based on longitudinal components that were very close to zero, indicating the importance of tidal dynamics in the region.

In the rainy season, the flows per unit area at the HE/ME interface (Fig. 4A) ranged between 1108.4 and 1563.4 m^{3}s^{-1} with an average of 1326.6 $\pm$ 158.1 m^{3}s^{-1}, whereas at the ME/LE interface (Fig. 4A), the flow rates ranged between 1721 and 2664.9 m^{3}s^{-1} with an average of 2195.1 $\pm$ 347.2 m^{3}s^{-1}. However, in the dry season at the HE/ME interface (Fig. 4B), the flow rates ranged between 72.4 and 174.6 m^{3}s^{-1} during the ebb tide, with an average of 132.8 $\pm$ 41.1 m^{3}s^{-1}, and between −181.9 and −287.4 m^{3}s^{-1} during the flood tide, with an average of −238.7 $\pm$ 34.6 m^{3}s^{-1}. At the ME/LE interface (Fig. 4B) at low tides, the values ranged between 109.4 and 578.2 m^{3}s^{-1} during the ebb tide, with an average of 335.2 $\pm$ 184.7 m^{3}s^{-1}, and between −445.2 and −617.1 m^{3}s^{-1} during the flood tide, with an average of −567.2 $\pm$ 64.1 m^{3}s^{-1}.

The net balance as a function of the flow rates in the rainy and dry seasons indicates that unidirectional flow occurred downstream of the estuary in the rainy season, corroborating the pattern of temporal variations in the currents (Fig. 4C). However, in the dry season, higher flow rates were observed during the flood tide, creating a flow of 328.5 m^{3}s^{-1} into the estuary, of which 202.4 m^{3}s^{-1} left the estuary during the ebb tide, which led to retention of 38% of the volume that entered during the flood tide.

4.3. Tidal prism and residence time

The highest river discharges occurred in the rainy season (Fig. 4). In addition, the drainage basin exported a total water volume of 55×10^6 m^3 to the estuary, which combined with the 42×10^6 m^3 present in the estuarine system (ME), resulted in the export of 97×10^6 m^3 of water to the ICS, with fresh water accounting for 99% of the discharge at both interfaces. The discharge rate observed in the rainy season at both interfaces was approximately 12 h.

In the dry season, the volume of water exported from the drainage basin to the estuary ranged between 5.9×10^6 and 11×10^6 m^3, and the percentages of freshwater during the ebb and flood tides were 80.0% and 75.7%, respectively. At the ME/LE interface, the water export volume ranged between 15×10^6 m^3 and 25×10^6 m^3, and the percentages of freshwater during the ebb and flood tides were 27.0% and 9.7%, respectively, demonstrating the greater influence of seawater at this interface. The rate of discharge ranged between 10.0 and 3.4 h during the ebb tide and between 9.4 and 1.2 h during the flood tide at the HE/ME and ME/LE interfaces, respectively.

Fig. 5 shows the tidal prism balance in the rainy and dry seasons. In the rainy season, the Jaguaribe River estuary behaved as water exporter based on its unidirectional flows, whereas in the dry season, the largest volumes were associated with the flood tide, generating retention of 4.9×10^6 m^3, which represented 36% of the input volume and indicates that the estuary was a water importer at this time of year. The difference between the volume of water that entered during the flood tide and the volume retained in the ME contributed to the transport of water to the ICS during the ebb tide. Moreover, there was a reduction in the volume transported seasonally: in the dry season, the average reduction was 84% at the HE/ME interface but only 52% at the ME/LE interface, indicating the great fluvial influence in the rainy season. The reduction in river volume clearly results in a decrease in the water volume transported to the estuary between the rainy and dry seasons, based on the decreases of 89% at the HE/ME interface and 64% at the ME/LE interface. A greater influence of seawater in the dry season was noted based on the analysis of the input volumes at these two interfaces, where the average transported volumes were 40%–47% higher, respectively.

4.4. Estuary type

In the rainy season, the average temporal variation in the velocity ($\overline{u}(t)$) in the water column reached 1 ms^{-1}, whereas the water level decreased 0.25 m throughout the day (Fig. 6A). At the ME/LE interface, even with a higher river volume, the average velocity (0.9 ms^{-1}) and the range in water levels (5.18–5.58 m) varied with the modulations in the semidiurnal tides (Fig. 6B). In addition, an average lag of 1 h between the maximum and minimum flows at flood and ebb tides and a difference between water velocities and water levels were observed. In the dry season, the change in water
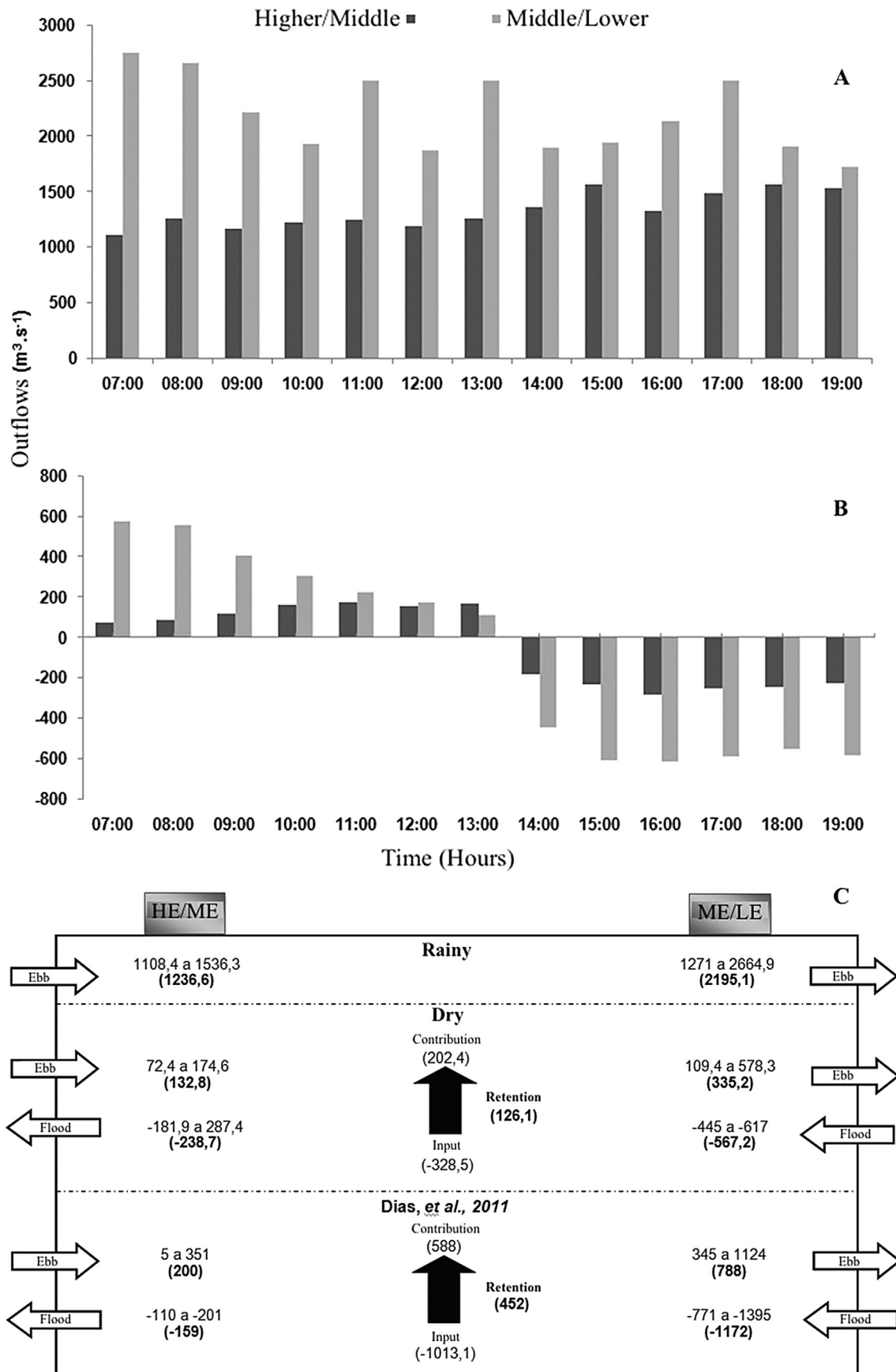
Fig. 4. Flows at the HE/ME and ME/LE interfaces in the Jaguaribe River estuary in the rainy season (A) and dry season (B) of 2009, and the net balance of water flows (m^3s^{-1}) at the HE/ME and ME/LE interfaces in the Jaguaribe River estuary in the rainy and dry seasons of 2009. The distance between the HE/ME and ME/LE interfaces was approximately 25 km, and the average depth was 4 m.

velocity and water level was associated much more with the semidiurnal variations in the local tides and at the HE/ME interface, the average height of the tide was 1.4 m, and there was an average lag of 1 h between maximum flows during the flood tide and minimum flow during the ebb tide (Fig. 6C). However, at the ME/LE interface, due to the asymmetry between the velocity and level curves, the measurement of the gap between the events was compromised because the curves did not show points of inflection between the ebb and flow tides (Fig. 6D).

Fig. 7 shows the tidal wave propagation and its effect on the salinity in the rainy and dry seasons. The asymmetry between the curves at both interfaces was generated by the river flow in the rainy season, based on the low salinity values. However, in the dry season, when the river flows were low, the average lag between minima and maxima was 3 h at the HE/ME interface (Fig. 7C), whereas at the ME/LE interface, the phase difference between the curves was 40 min (Fig. 7D). This pattern indicates that the propagation of high salinity when entering the estuary is affected by the river flow downstream of the estuary, causing a lag in relation to the dynamic tide. The interaction between the tidal wave, which propagates upstream of the estuary, and the local morphology is responsible for the rise in tidal height and the increase in current intensities. The rise in tidal height is related to the narrowing of the estuary channel at the HE/ME interface and stronger side and bottom friction, which raise tidal heights in this area.

Fig. 7 E–H shows the influence of the propagation of the barotropic tide. Fig. 7 A–D shows that in the rainy season, there was a strong asymmetry between variations in the tide and salinity, which were generated by the higher river flow, whereas in the dry season, the semidiurnal modulation of the tide controlled the entry of the tidal wave into the estuary channel. This seasonal difference suggests that the redistribution of salinity is caused exclusively by the advective effect of the tide because during the flood tide, the salinity gradually increases upstream of the estuary to the inner limit of the ME, whereas during the ebb tide, the salinity decreases because of the higher amount of freshwater stored during the flood tide. Therefore, the saline wave in a given longitudinal position lags approximately 3 h behind the tide and currents; this pattern was observed during a period of low river flow at the ME in the Jaguaribe River estuary.

The data plotted on the stratification–circulation diagram of Hansen and Rattray (1986) show that in the rainy season, due to the low salinity, it was not possible to classify the estuarine system (Fig. 8). However, in the dry season, the estuary was a type 2a system (partially mixed and with weak vertical stratification) in which gravitational movement was virtually nonexistent and the transport of substances from upstream of the estuary was virtually all due to turbulent diffusion. The value $\gamma = 0.99$ indicates a transition between types 2a and 1a (well mixed).

Due to the high river discharge in the rainy season, it was not possible to calculate the estuarine Richardson number (Ri). However, in the dry season, the Ri was 6.1 during the tidal cycle. Fig. 8B shows the temporal variation in the Richardson number by layer (RiL). The RiL values indicate a condition of weak vertical stability (usually RiL > 2) in the rainy season, when the estuary was strongly influenced by river discharge. The RiL values corresponding to the dry season were generally lower than 2, indicating conditions of vertical instability and the predominant influence of the tides.

The distribution of RiL values at the two interfaces indicates that at the HE/ME interface in the rainy season (Fig. 8B-1), none of the values indicate a condition of high stability (RiL > 20). Most of the data indicate weak vertical stability (2 < RiL < 20) and occasional instability (RiL < 2), which was also observed at the ME/LE interface. The variation in RiL at both interfaces confirms the unidirectionality of river flow in the rainy season and its homogeneity. In

the dry season, all values were less than 2 (RiL < 2), indicating vertical instability due to increased tidal activity during this period. In the dry season, when the kinetic energy of the tides more strongly affected the estuary dynamics, RiL values varied within the range of high vertical instability, indicating a condition of high vertical mixing and the high influence of turbulent mixing.

4.5. Materials and net transport

Tidal currents, gravity flow, and river discharge are the three forces responsible for the advective transport of salt in estuarine systems. The first two operate upstream of the estuary, and the third force is responsible for the transport to the continental shelf. However, in partially mixed estuaries with weak vertical stratification (type 2a) and in well-mixed estuaries (type 1a), salt is transported upstream to the estuary predominantly via gravity flow and tidal propagation.

In the rainy season (Fig. 9), the transport of salt was predominantly associated with advective processes (river discharge) at the HE/ME (Fig. 9A) and ME/LE (Fig. 9B) interfaces, demonstrating the strong fluvial influence. In the dry season, the fluvial component caused salt transport upstream of the estuary (1.6 kg m^{-1}s^{-1}) at the HE/ME interface (Fig. 9C), whereas transport was downstream of the estuary with similar values at the ME/LE interface (Fig. 9D). The transport associated with Stokes drift was greater at the ME/LE interface, reaching values of 3.5 kg m^{-1}s^{-1}, although its orientation indicated transport upstream of the estuary (diffusive nature), whereas the expected theoretical pattern was in the opposite direction. The transport associated with Stokes drift corresponds to mass transport generated by the tidal propagation in the estuary. Advective transport of salt downstream of the estuary generated by tides at the HE/ME interface was 4.8 kg m^{-1}s^{-1} whereas this transport was upstream of the estuary at the ME/LE interface (3.7 kg m^{-1}s^{-1}). At both interfaces, salt transport related to tides was directed toward the ME. Salt accumulation at the ME may result in months of negative water balance and hypersalinization of the ME, thereby changing the orientation of the longitudinal baroclinic component of the pressure gradient force per unit mass, which is typically oriented upstream.

Another type of transport that was evaluated is that associated with residual currents. In the rainy season, due to the large river discharge, no transport associated with this component was observed. However, in the dry season, the transport by residual currents was similar to that of the tidal currents and reached 4.8 kg m^{-1}s^{-1} at the HE/ME interface and 4 kg m^{-1}s^{-1} at the ME/LE interface. The transport of salt toward the ME in the Jaguaribe River estuary became evident in these analyses. The resulting salt transport in the rainy season was 0.23 kg m^{-1}s^{-1} at the HE/ME interface and 0.65 kg m^{-1}s^{-1} at the ME/LE interface. In the dry season, the resulting transport was approximately 8 kg m^{-1}s^{-1} downstream of the estuary and reached 9 kg m^{-1}s^{-1} at the ME/LE interface. The transport of salt associated with the river discharge was more strongly influenced by tides at the HE/ME interface in the dry season due to the greater storage of freshwater during the tidal cycle, whereas at the ME/LE interface, the pattern was closely associated with tidal modulation, and this pattern is corroborated by the transport generated by the tidal currents.

The spatial distribution of SPM in the Jaguaribe River estuary in the rainy season (Fig. 10A) indicates that the highest concentration of SPM was present along the estuary channel and ranged between 66.8 and 75.4 mgL^{-1} with an average of 72.3 mg.L^{-1} at the HE/ME interface. At the ME/LE interface, the observed concentration of SPM ranged between 54.8 and 81.4 mgL^{-1} with an average of 74.8 mgL^{-1}. In the ICS, the concentration ranged between 21.9 and 62.2 mgL^{-1} with an average of 39.7 mgL^{-1}. The high concentration
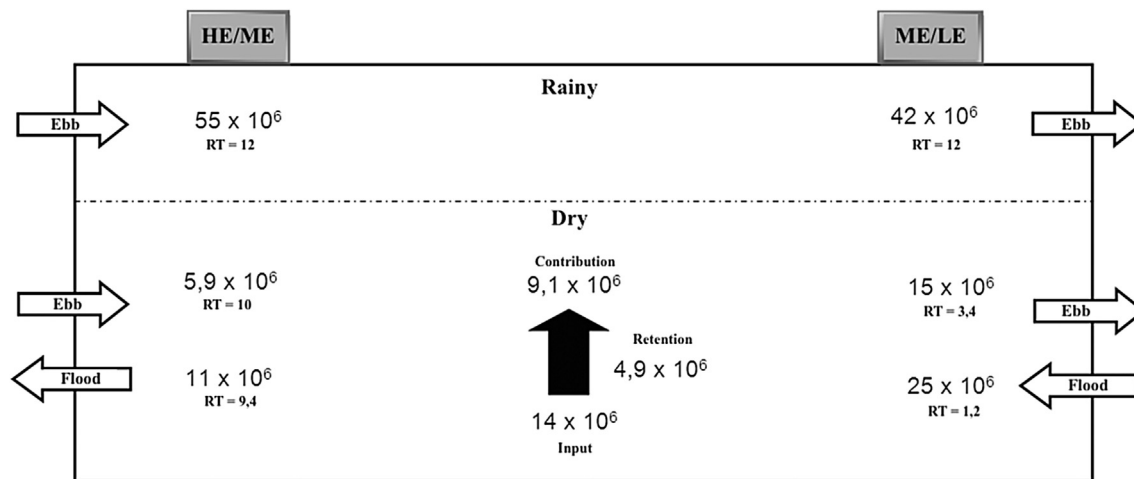
Fig. 5. Tidal prisms at the HE/ME and ME/LE interfaces in the Jaguaribe River estuary in the rainy and dry seasons of 2009. The tidal prism and residence time (RT) are expressed in m^3 and hours, respectively. The distance between the HE/ME and ME/LE interfaces was approximately 25 km, and the average depth was 4 m.
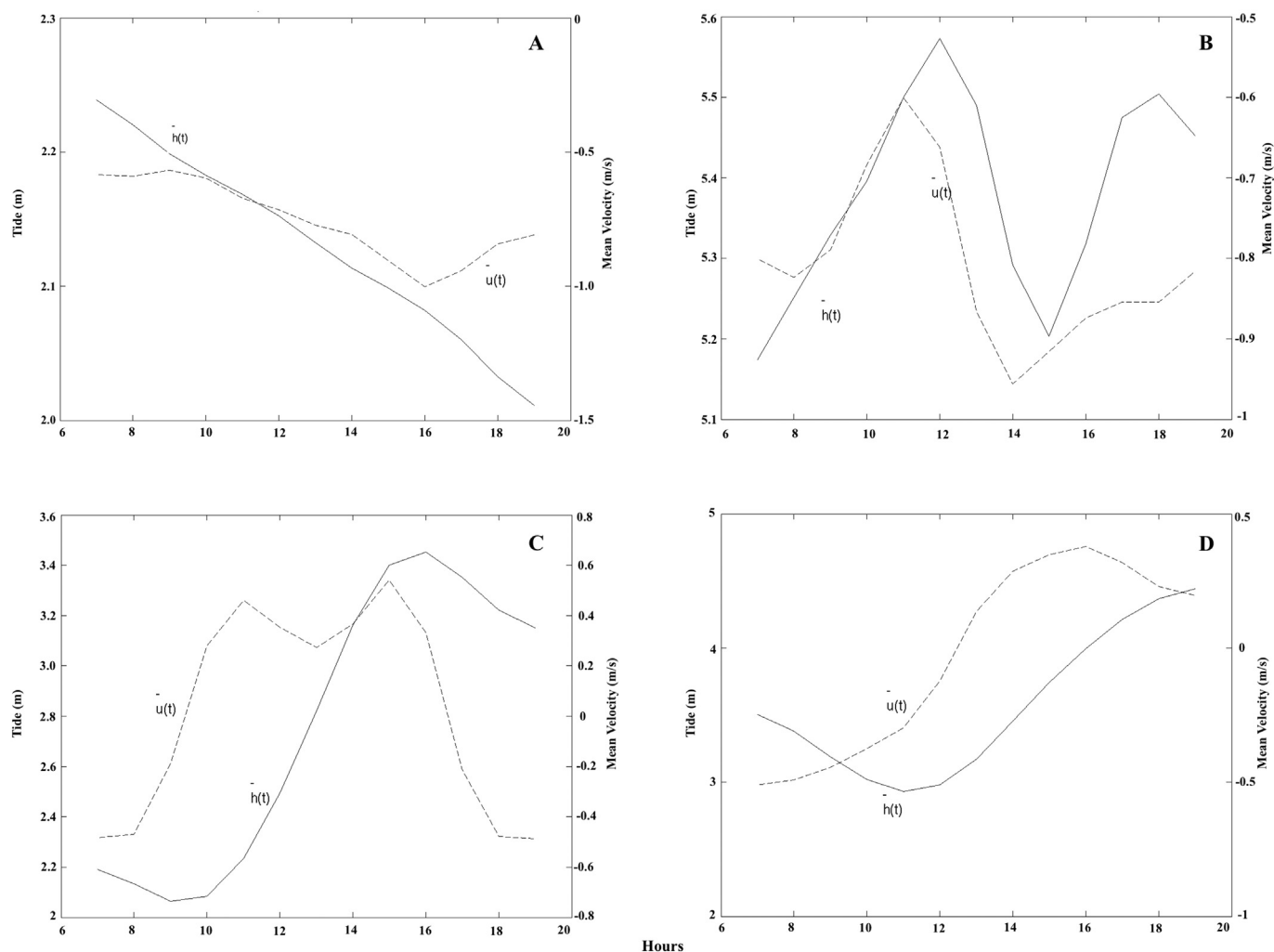

Fig. 6. Temporal variations in the average velocity [$\overline{u}(t)$] in the water column (dotted line) and the tide [h(t)] (solid line). HE/ME (A) and ME/LE (B) interfaces in the rainy season and HE/ME (C) and ME/LE (D) interfaces in the dry season.

of SPM is associated with the increased water volume observed during this season, which produced an SPM plume in the ICS.

In the dry season, the SPM concentration ranged between 11.7 and 20.6 mgL^{-1} with an average of 18.2 mgL^{-1} at the HE/ME
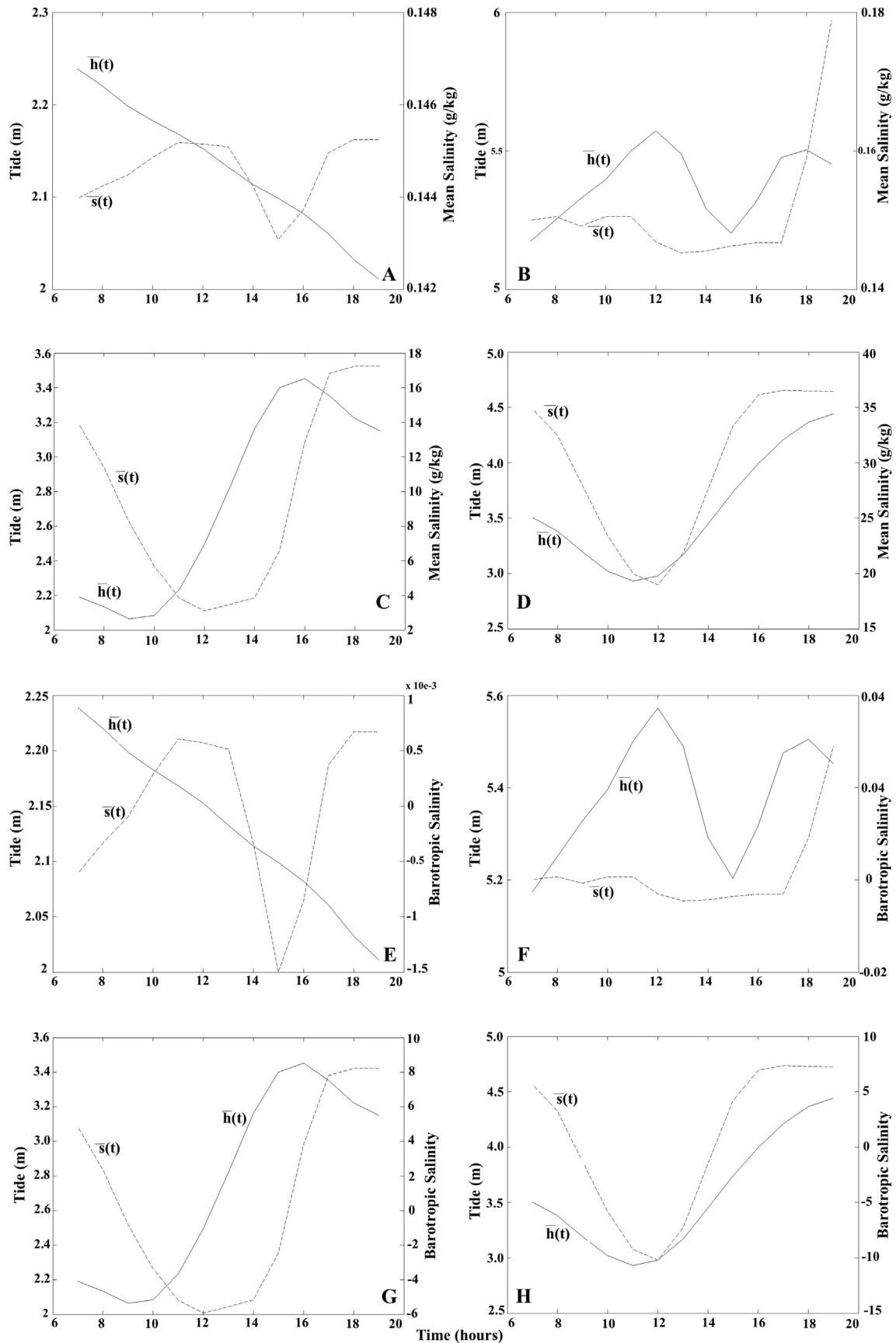
Fig. 7. Average temporal variations in salinity [S(t)] in the water column (dotted line) and tide [h(t)] (solid line). HE/ME(A,E) and ME/LE (B,F) interfaces and HE/ME(C,G) and ME/LE (D,H) interfaces in the rainy and dry seasons of 2009.
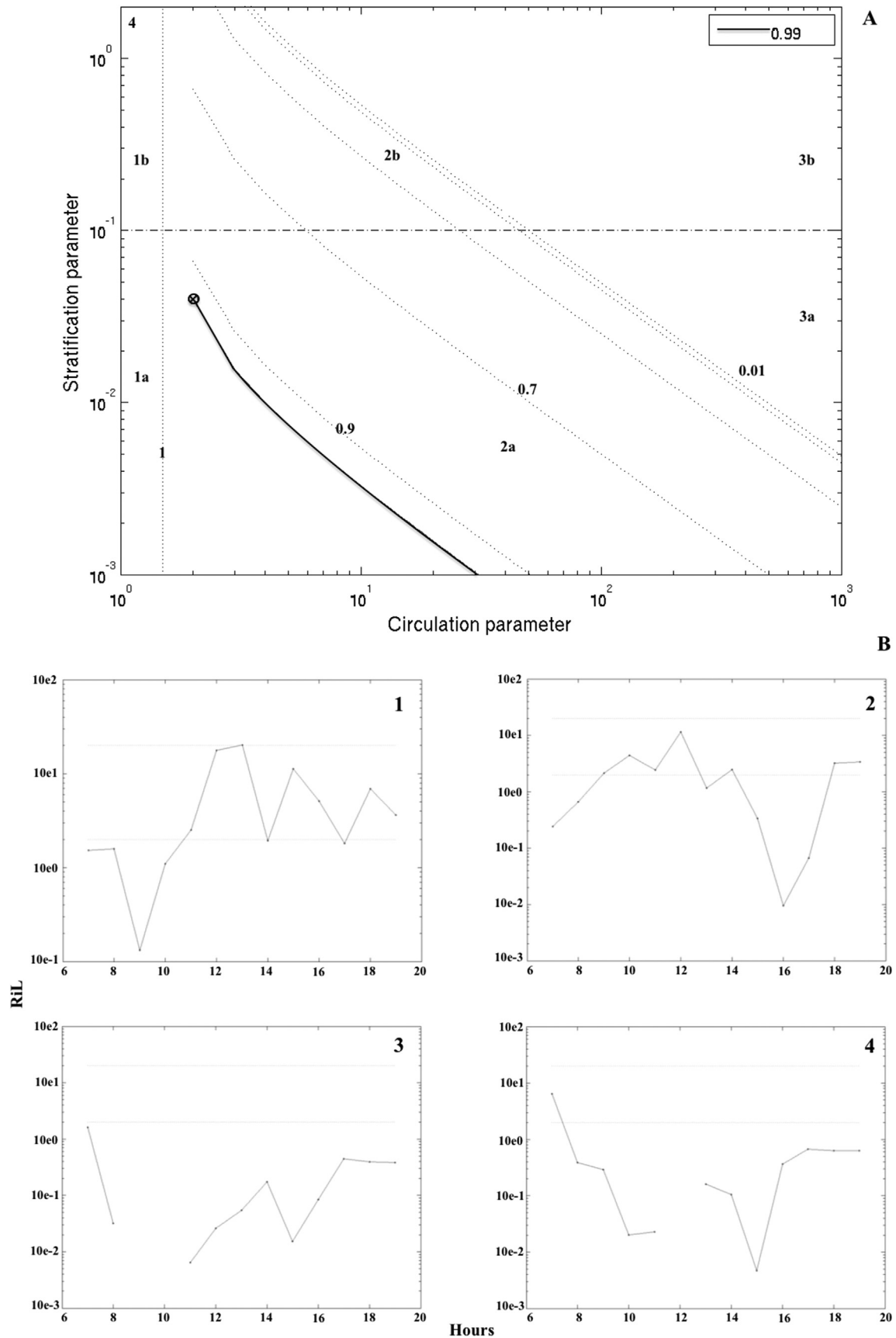
Fig. 8. A - Parametric curve relative proportion ($0 \leq \gamma \leq 1$) of advective and dispersive processes of the Jaguaribe River estuary in 2009. B - Temporal variations in the Richardson numbers corresponding to layers. The dashed lines delineate the following: RiL >20, which indicates high stability (upper line); 2 < RiL < 20, which indicates weak vertical stability; and RiL < 2, which indicates vertical instability (bottom row). HE/ME(1) and ME/LE (2) interfaces in the rainy season and HE/ME(3) and ME/LE (4) interfaces in the dry season.

interface and between 15.2 and 52.9 mgL^{-1} with an average of 29.6 mgL^{-1} at the ME/LE interface. In the ICS, the SPM concentration ranged between 18.7 and 47.7 mgL^{-1} with an average of 28 mgL^{-1}. The lowest SPM concentration was observed at the HE/ME interface (Fig. 10B), and these concentrations increased to 58.5 mgL^{-1} at the ME/LE interface. However, during the flood tide (Fig. 10C), because of the lower river intake and increased activity of seawater, the SPM concentration ranged between 52.8 and 58.5 mgL^{-1}.

The lowest SPM concentrations were observed in the dry season, influenced by the modulation of the local tide. At low tide (Fig. 10B), the highest SPM concentration occurred near the mouth of the Jaguaribe River, in the influence area of the LE. When the tide began to rise (Fig. 10C), the highest concentration extended to the inner area of the ME. In the transition between the HE/ME interfaces, there was a region where the velocities resulting from converging movements, river discharge, and tidal propagation were practically nil, resulting in the higher SPM concentration and a zone of maximum turbidity, which was mapped for the first time in the Jaguaribe River estuary.

The SPM concentration decreased by averages of 72% at the HE/ME interface and 21% at the ME/LE interface in the dry season compared with the rainy season because of the lower river intake and increased activity of seawater in the dry season, when the zone of maximum turbidity formed in the ME. Even in the dry season, the SPM concentration in this area was approximately that of the seawater, and the measured SPM concentration in the ME was very similar to that observed in the rainy season due to resuspension of bottom material, erosion of margins, or changes in sources. During periods of greater river discharges, the drainage basin transported 2.9×10^6 tons of water per year to the estuary, whereas at the ME/LE interface, the average discharge was 2.0×10^6 tons.year^{-1}, resulting in an average export of 4.9×10^6 tons.year^{-1} to the ICS. In the dry season at low tide, the SPM discharges at the HE/ME interface were 0.1×10^6 tons.year^{-1}, whereas at the ME/LE interface, they reached 0.41×10^6 tons.year^{-1}, indicating that significant sources of SPM are present in the ME. At flood tides, the flow rates were 1.1×10^6 tons.year^{-1} at the ME/LE interface and 0.13×10^6 tons.year^{-1} at the HE/ME interface, suggesting that SPM is transported to the continent, which supports the creation of new areas of sedimentation and colonization by mangroves, as observed by Godoy and Lacerda et al. (2014).

Of the total flow of SPM that entered the estuary system during the flood tides at the ME/LE interface, 32% contributed to the discharge of SPM at ebb tides, and the remainder was retained in the ME. This pattern suggests that the Jaguaribe River estuary during the study period was an exporter of material in the rainy season and an importer of material during the period of decreased fluvial activity such that more than 60% of the SPM flow was retained in the ME.

5. Discussion

The unidirectional flows at the HE/ME and ME/LE interfaces indicate that in the dry season, there is a greater influence of marine waters in the estuary system, which results in flood flows that are greater than those at ebb tides at both interfaces. This influence suggests that the dams upstream of the estuary played an important role in the availability of water to the coast in the dry season.

The profiles of stationary velocities u$_a$ at the HE/ME and ME/LE interfaces (Fig. 3) revealed the fluvial influence in the estuarine system. Positive values of u$_a$ at the HE/ME interface (0.76 ms^{-1}) and ME/LE interface (0.81 ms^{-1}) in the rainy season indicate the transport downstream of the estuary and that the system is a water exporter during periods of unidirectional flows, corroborating the

results of Dias et al. (2011, 2013a,b). The gravity flow downstream of the estuary in the dry season at the HE/ME interface and upstream of the estuary at the ME/LE interface suggests that seawater volumes that enter the estuary system during flood tide are similar to those that leave at ebb tide, with stationary velocities of approximately zero.

The water export from the estuary in the rainy season had a strong fluvial contribution in the rainy season and continually generated positive water current velocities (downstream of the estuary) at the HE/ME and ME/LE interfaces, and this pattern was also observed during the ebb tide in the dry season. However, in the dry season, the gravity flow associated with flood velocities indicate the importance of the marine component in the renewal of the estuarine water mass and that the estuary is a water importer in this season.

Nicolite et al. (2009) observed that the water level and low current velocities in the low estuary of the Paraíba do Sul River during periods of moderate river discharge (within the historical average) were dominated by the co-oscillation of the tide, and the river discharge had a stronger influence on the current levels and velocities at low tide. This pattern was also observed in the Jaguaribe River estuary in the dry season. However, the authors note that during periods of high river discharge (>1500 m^{3}s^{-1}), the water levels were strongly influenced by the river discharge and by the semidiurnal variation of the tide. This pattern was not observed in the Jaguaribe River estuary in the rainy season because the zone of mixing had been advected beyond the estuary to the ICS. Andutta et al. (2013) reported that the Peruípe River estuary, located in the state of Bahia, Brazil, displayed behavior similar to that of the Jaguaribe River estuary, where the river flows dominate the estuary discharges only in the rainy season.

The calculated Ri was 6.1 during a tidal cycle, indicating that the estuary was strongly dominated by high river discharges in the rainy season, whereas tidal energy was the major force, along with minor river discharge, in the dry season. The observed values of RiL in the rainy season oscillated within the range of weak vertical stability and occasionally indicated instability, and thus, the river flows were unidirectional. In the dry season, when the tidal energy dominated the estuary dynamics, the RiL numbers fluctuated within the range of high vertical instability, indicating extensive mixing and a large contribution of turbulent mixing processes.

Andutta (2006) reported that in the Curimataú River estuary (state of Rio Grande do Norte, Brazil), due to high variations in river flows, stratification extended into neap tides associated with low velocities during ebb currents, and advective transport of salt measured 7.3 kg m^{-1}s^{-1}. However, the weak vertical stratification and semidiurnal modulation of tidal currents during syzygy occurred in response to a decrease in the entry of freshwater into the estuary system on a time scale of approximately 6–7 days.

In the rainy season, the volume of water in the Jaguaribe River estuary system was approximately 97×10^6 m^3, fresh water accounted for 99% of the volume, and the RT was approximately 12 h. In the dry season, the volume exported during the ebb tide was lower than the volume imported during the flood tide. However, during the ebb tide, the freshwater percentages were approximately 78%, whereas during the flood tide, they ranged between 9% and 27%. Smaller RTs of approximately 1.2 h were observed at the ME/LE interface during the flood tide. Dias et al. (2011) studied the Jaguaribe River during spring tide and observed that the total volume of water at the HE/ME interface was 12×10^6 m^3 with a freshwater percentage of 24% and a discharge time of 3 h, whereas at the ME/LE interface, the observed volume was approximately 3-fold higher than that observed at the HE/ME interface and reached 43×10^6 m^3, with a freshwater percentage of only 5.9% and a flushing time of 0.7 h.
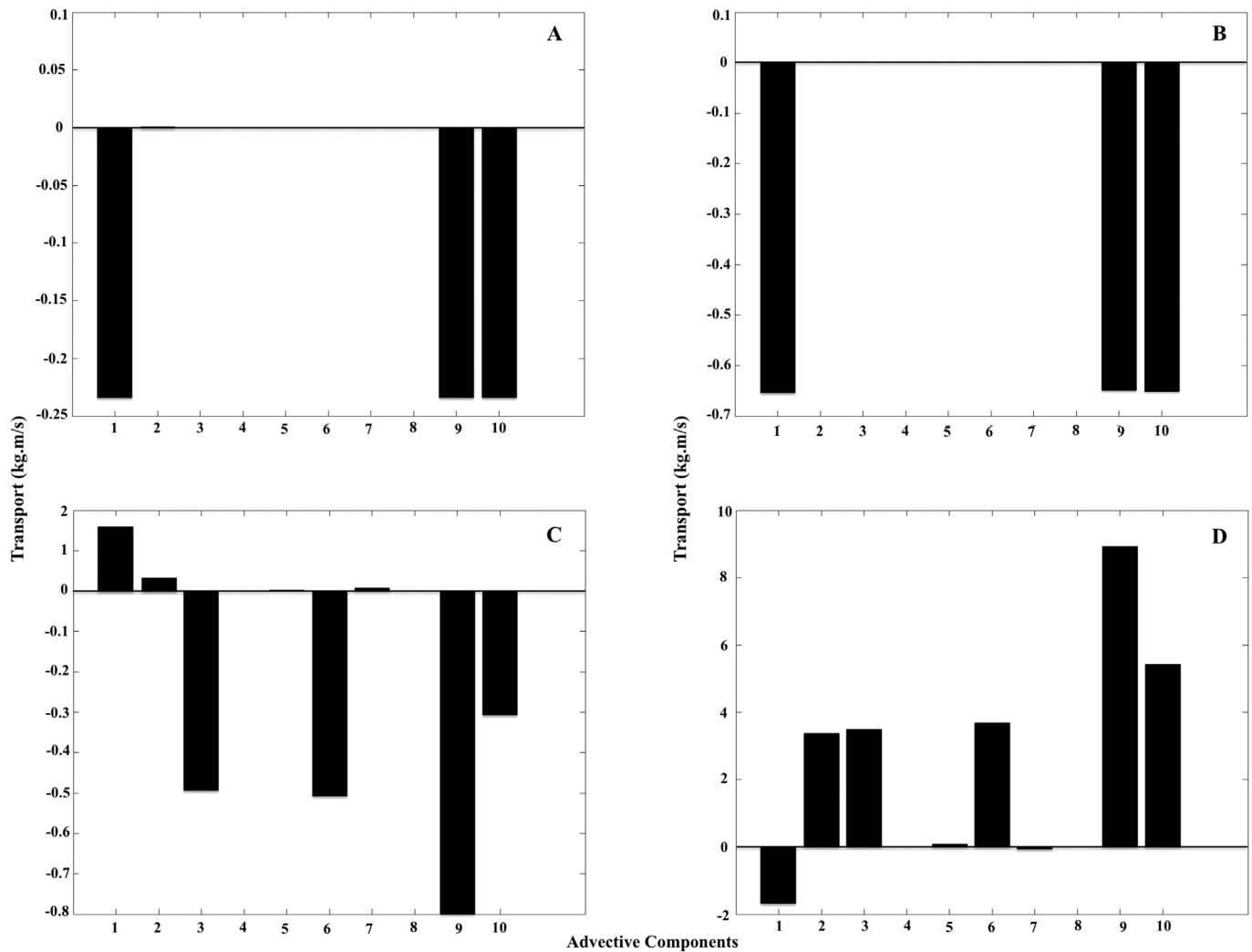
Fig. 9. Advective transport of salt associated with river discharge (1), Stokes drift (2), tidal currents (3), gravity flow (4), turbulent fluctuations (5), residual currents (6), and triple correlation (7). Histograms (9) and (10) show the calculated transport obtained from equation (13) and the sum of its components. HE/ME(A) and ME/LE (B) interfaces in the rainy season and HE/ME(C) and ME/LE (D) interfaces in the dry season.

Therefore, the change in the salinity curve over time at a given longitudinal position will lag approximately 3 h behind the dynamic tide curve; this pattern was observed during a period of low river flow in the Jaguaribe River estuary in the MZ. The data plotted on the stratification−circulation diagram of Hansen and Rattray (1986) show estuary system values of γ of approximately 0.99, indicating that the estuary is at the transition between types 2a (partially mixed and with weak vertical stratification) and 1a (well mixed). Similar findings were reported by Izumi (2011) in the Caravelas River estuary, Bahia, Brazil, and those authors noted that turbulent diffusion is the primary mechanism responsible for the transport of salt and other materials. Andutta (2006) studied the Curimataú River estuary, Rio Grande do Norte, and classified the estuary during tidal and spring tides as a type 2b (highly stratified) system, indicating the dominance of tidal diffusion at these two times. Andutta et al. (2013) concluded that the Peruípe River estuary changed from partially mixed and highly stratified (2b) during spring tides to highly stratified (1b) during neap tides. This pattern is similar to that observed in the estuaries of the Curimataú and Jaguaribe Rivers because of the dominance of river discharge during neap tides in the Curimataú and in the rainy season in the

Jaguaribe, where conditions varied between stability and weak vertical stability, respectively. During spring tides (the dry season), the strongest influence of the tide generated vertical instability in both estuaries.

Because of this pattern, the tidal transport of salt at the HE/ME and ME/LE interfaces was toward the ME. Salt accumulation in the ME may result in months of negative water balance in relation to hypersalinization of the estuary. The hypersalinization of some areas of the estuary was observed by Marins et al. (2003), who classified the estuary as negative. This reversal leads to the greater permanence of seawater that enters the estuary system during flood tides and increases the RT, providing ideal conditions for the accumulation of nutrients and SPM of aquagenic or biogenic origin. This accumulation can enhance eutrophication and flocculation in this area, where evaporation rates are high. Andutta (2006) concluded that salt transport to the Curimataú River estuary was predominantly driven by river discharges and the advective effect of Stokes drift. Schettini and Miranda (2010) studied the Caravelas River estuary and observed that the transport was greater during spring tides than neap tides when combined with decreased seasonal river discharges. In the rainy season, this transport was
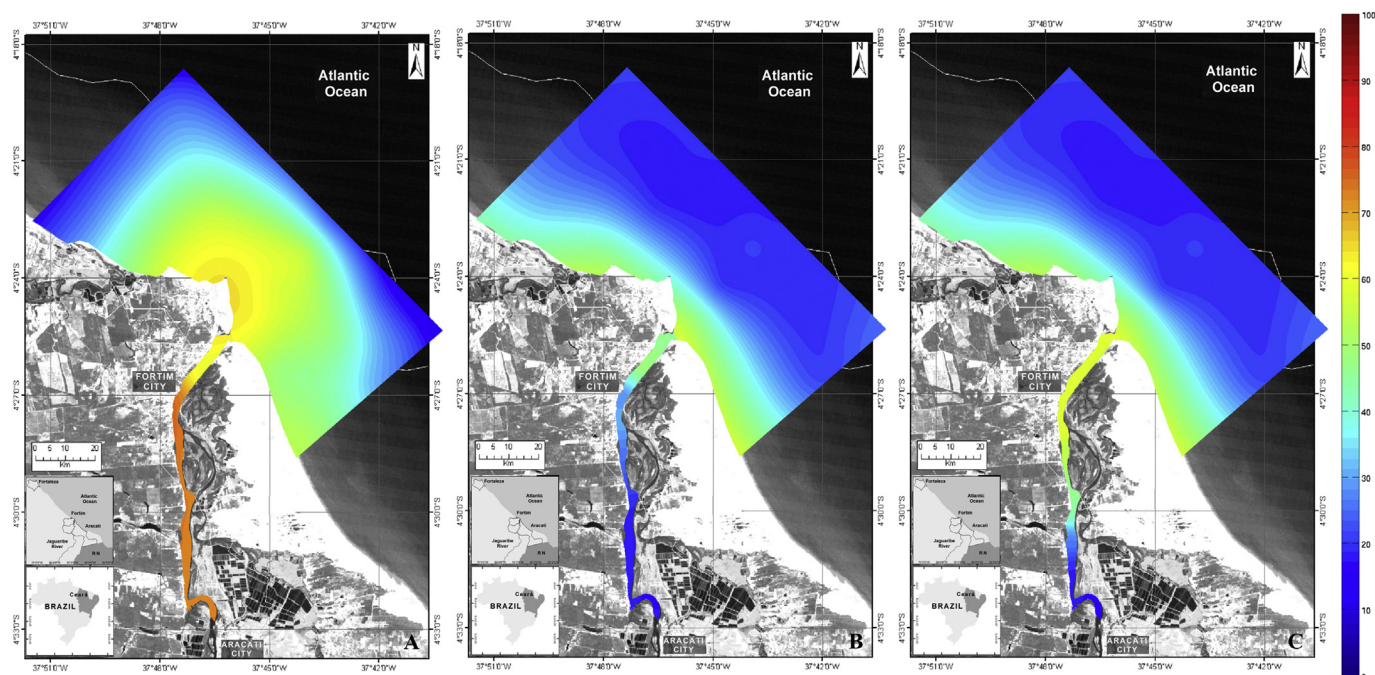
Fig. 10. Distribution of suspended particulate matter (SPM mg.L^{-1}) in the Jaguaribe River estuary (HE/ME and ME/LE) and inner continental shelf (ICS) during the rainy season (A), at ebb tides (B) and flood tides (C) in the dry season of 2009. HE/ME (37°47′22″ W/4°32′20″ S) and ME/LE (37°47′35″ W/4°27′00″ S).

primarily associated with Stokes drift. This behavior observed in the Caravelas River estuary is consistent with the results obtained in this study related to the advective transport due to variations in river discharge.

The comparison of the average concentrations of SPM in the ICS and at the ME/LE interface during flood tides indicates that much of the SPM present in the ME is of marine origin or is the result of erosion of margins and the reworking of bottom material. The SPM balance in the Jaguaribe River estuary involves the export of materials in the rainy season and the retention of SPM in the ME between ebb and flood tides during the dry season. The spatial mapping of the turbidity maximum zone is rarely reported in studies of estuarine systems in northeastern Brazil. Its location can lead to understanding of oxygen consumption processes, modification of organic matter and export of CO_2 to the Equatorial Atlantic. The physical understanding of the behavior of intensively dammed rivers, as is the case of the Jaguaribe River, is of fundamental importance and relevance in the face of local and global climate change scenarios.

6. Conclusions

In the rainy season, the estuarine discharge was predominantly fluvial, and there were small variations in vertical and partly mixed gradients. In the dry season, continental waters predominated during the ebb tide, and during the flood tide, seawater was imported and vertical gradients changed to a pattern of greater water mixing.

The high river volume was transported predominantly unidirectionally and longitudinally in the rainy season and bidirectionally in the dry season, when the transverse transport in the estuary decreased sharply. This transport caused a tidal delay of approximately 3 h.

The resulting flow rates were one order of magnitude higher in the rainy season. Control of the estuary by tidal modulation in the dry season caused a net retention of more than 65% of the volume at the HE/ME interface and led to RTs of more than 9 h during the flood and ebb tides, whereas in the rainy season, even with the increased export of river water, the RT lengthened to 12 h.

Tidal modulation in the dry season led to a maximum zone of turbidity due to the trapping of the estuary water by the tide and most likely to the concentration of certain substances, which may have intensified the effects of anthropogenic alteration of discharges. The freshwater flow of 80% in the rainy season decreased to less than 10% in the dry season, reflecting the local seasonality of the climate.

This study showed that in estuaries in northeastern Brazil, including those with a strong control of the natural flow regime as in the Jaguaribe River, dams tend to cause diffusive processes associated with the baroclinic effect, such as the mechanisms responsible for the transport of substances at the continent–ocean interface. In the Jaguaribe River, the decrease in river flow during the dry season is a cause for concern because this decrease significantly changes the transport of materials to the ocean, highlighting the need for the constant monitoring of the river properties and the current fields to develop a set of environmental strategies for better management of this important coastal ecosystem and maintenance of its ecological functions.

References

ANA, 2006. Vazões históricas para a bacia de drenagem do rio Jaguaribe (CE). In: Relatório interno. Brasília: Agência Nacional de Água - SP, p. 20.

Andutta, F.P., 2006. Experimentos e Modelagem Numérica com Aplicação ao Estuário Tropical do Rio Curimataú, RN (Msc thesis). Universidade de São Paulo, São Paulo, p. 140.

Andutta, F.P., Miranda, L.B., Schettini, C.A., Siegle, E., da Silva, M.P., Izumi, V.M., Chagas, F.M., 2013. Temporal variations of temperature, salinity and circulation in the Peruípe river estuary (nova Viçosa, BA). Cont. Shelf Res. 70, 36—45.

Aurenhammer, F., Klein, R., 1989. Voronoi Diagrams. 1a. ed. FernUniversität Hagen: Technical Report, p. 92.

Bergamo, A.L., Miranda, L.B., Correa, M.A., 2002. Estuário: programas para processamento e analise de dados hidrográficos e correntográficos. Relatório Técnico do Inst. Ocean. 49, 1—16.

Campos, J.N.B., Studart, T.M., Luna, R., Franco, S., 2000. Hydrological transformations in jaguaribe river basin during 20th century. In: Proceedings of the 20th Annual American Geophysical Union. Hydrology Days Publications, pp. 221—227.

Delandmeter, P., Lews, A.E., Lambrechts, J., Deseersnijder, E., Legat, V., Wolanski, E., 2015. The transport and fate of riverine fine sediment exported to a semi-open system. Estuar. Coast. Shelf Sci. 167, 336e346.

Dias, F.J.S., Castro, B.M., Lacerda, L.D., 2013a. Continental shelf water masses off the Jaguaribe River (4 S), Northeastern Brazil. Cont. Shelf Res. 66, 123—135.

Dias, F.J.S., Marins, R.V., Maia, L.P., 2013b. Impact of drainage basin changes on suspended matter and particulate copper and zinc discharges to the ocean from the Jaguaribe River in the semiarid NE Brazilian coast. J. Coast. Res. 290, 1137—1145.

Dias, F.J.S., Lacerda, L.D., Marins, R.V., de Paula, F.C.F., 2011. Comparative analysis of rating curve and ADP estimates of instantaneous water discharge through estuaries in two contrasting Brazilian rivers. Hydrol. Process. 25, 2188—2201, 2011.

Dias, F.J.S., Marins, R.V., Maia, L.P., 2009. Hydrology of a well-mixed estuary at the semi-arid Northeastern Brazilian coast. Acta Limnol. Bras. 21, 377—385.

Dias, F.J.S., 2007. Hidrodinâmica das descargas fluviais para o estuário do Rio Jaguaribe (CE). 125 p (Msc thesis). Universidade Federal do Ceará - Instituto de Ciências do Mar - LABOMAR, Fortaleza.

Dyer, K.R., 1974. The salt balance in stratified estuaries. Estuar. Coast. Mar. Sci. 2, 273—281.

Dyer, K.R., 1986. Coastal and Estuarine Sediment Dynamics. John Wiley and Sons, New York, p. 342.

Dyer, K.R., 1987. Estuaries: a Physical Introduction, second ed. John Wiley and Sons, New York, p. 195.

Emery, W.J., Thomson, R.E., 2001. Data Analysis Methods in Physical Oceanography. Elsevier Science, Amsterdam, 2001, Pages xi-xii, ISBN 9780444507563. http://dx.doi.org/10.1016/B978-044450756-3/50000-9. http://www.sciencedirect.com/science/article/pii/B9780444507563500009.

Fabricius, K.E., Death, G., Humphrey, C., Zagorskis, I., Schaffelke, B., 2013. Intraannual variation in turbidity in response to terrestrial runoff on near-shore coral reefs of the Great Barrier Reef. Estuar. Coast. Shelf Sci. 116, 57e65.

Fabricius, K.E., Logan, M., Weeks, S., Brodie, J., 2014. The effects of river run-off on water clarity across the central Great Barrier Reef. Mar. Pollut. Bull. 84 (1), 191e200.

Fettweis, M., Sas, M., Monbaliu, J., 1998. Seasonal, neap—spring and tidal variation of cohesive sediment concentration in the Scheldt estuary. Belg. Estuar. Coast. Shelf Sci. 47, 21—36.

Flores, F., Hoogenboom, M.O., Smith, L.D., Cooper, T.F., Abrego, D., Negri, A.P., 2012. Chronic exposure of corals to fine sediments: lethal and sub-lethal impacts. PloS One 7, e37795.

French, J.R., Burningham, H., Benson, T., 2008. Tidal and meteorological forcing of suspended sediment flux in a muddy mesotidal estuary. Estuaries Coasts 31, 843—859.

Funceme, 2010. Precipitações históricas para o baixo Jaguaribe. Eletronic J. www.funceme.br/monitoramento/graficosdechuvas Acess in 10 march 2010.

Godoy, M.D., Lacerda, L.D., 2013. Changes of estuarine and islands rainfall tendencies in the Jaguaribe River watershed — CE, Brazil. Mar. Sci. Files 46, 47—54.

Godoy, M.D.P., Lacerda, L.D., 2015. Mangroves response to climate change: a review of recent findings on mangrove extension and distribution. An. Acad. Bras. Ciências (Impresso) 87, 651—667.

Hansen, D., Rattray, M.J., 1986. New dimensions in estuary classification. Liminol. Oceanogr. 11 (3), 319—325.

Hunkins, K., 1981. Salt dispersion in the hudson estuary. J. Phys. Oceanogr. 11, 729—738.

IBGE- Instituto Brasileiro de Geografia e Estatística, 2014. Estimativas da População dos Municípios Brasileiros com Data de Referência em 1º de julho de, p. 2014.

Izumi, V.M., 2011. Comparação entre as desembocaduras do Complexo Estuarino do Cassurubá (BA): Características hidrográficas e hidrodinâmicas (MSc thesis).

Ketchum, B.H., 1950. Hydrografic factors involved in the dispersion of pollutants intro- duced into tidal wateres. J. Boston Soc. Civ. Eng. 37, 296—314.

Kjerfve, B., 1975. Velocity averaging in estuaries characterized by a large tidal range to depth ratio. Estuar. Coast. Mar. Sci. 3, 311—323.

Lacerda, L.D., Costa, B.G.B.C., Lopes, D.N., Oliveira, K., Bezerra, M.F., Bastos, W.R., 2014. Mercury in indigenous, introduced and farmed fish from the semiarid region of the Jaguaribe River basin, NE Brazil. Bull. Environ. Contam. Toxicol. 93, 31—35.

Lacerda, L.D., Dias, F.J.S., Marins, Rozane V., Soares, T.C.M., Godoy, J.M., Godoy, M.L.D.P., 2013. Pluriannual watershed discharges of Hg into a tropical semi-arid estuary of the Jaguaribe River, NE Brazil. J. Braz. Chem. Soc. (Impresso) 24, 1719—1731.

Lacerda, L.D., Marins, R.V., Dias, F.J.S., Soares, T.M., 2012. The arctic paradox: impacts of climate changes on rivers from the arctic and the semiarid increase mercury export to the ocean. Rev. Virtual Quím. 4, 456—463.

Ludwig, W., Probst, J.L., Kempe, S., 1996. Predicting the oceanic input of organic carbon by continental erosion. Glob. Geochem. Cycles 10, 23—41.

Luketina, D., 1998. Simple tidal prism models revisited. Estuar. Coast. Shelf Sci. 46, 77—84.

Maia, L.P., Lacerda, L.D., Monteiro, L.H.U., Souza, G.M.E., 2006. Atlas dos Manguezais do Nordeste; Avaliação das Áreas de Manguezal dos Estados do Piauí, Ceará, Rio Grande do Norte, Paraíba e Pernambuco. Fortaleza Supt. Estadual do Meio Ambiente 1, 125.

Marins, R.V., Lacerda, L.D., Abreu, I.M., Dias, F.J.S., 2003. Efeitos da açudagem no rio Jaguaribe, vol. 33. Ciência Hoje, Rio de Janeiro n.197, p. 66—70.

Marins, R.V., Paula Filho, F.J., Eschrique, S.A., Lacerda, Ld., 2011. Anthropogenic sources and distribution of phosphorus in sediments from the Jaguaribe River estuary, NE, Brazil. Braz. J. Biol. (Impresso) 71, 673—678.

Milliman, J.D., Farnsworth, K.L., 2011. River Discharge to the Coastal Ocean: a Global Synthesis. Cambridge University Press.

Miranda, L.B., Bérgamo, A.L., Castro, B.M., 2005. Interactions of river discharge and tidal modulation in a tropical estuary, NE Brazil. Ocean. Dyn. 55, 430—440.

Miranda, L.B., Castro, B.M., Kjerfve, B., 2002. Princípios de Oceanografia Física de Estuários. Universidade de São Paulo, São Paulo, p. 414.

Nicolite, M., Trucollo, E.C., Schettini, C.A.F., Carvalho, C.E.V., 2009. Oscilação do nível de água e co-oscilação da maré astronômica no baixo estuário do rio Paraíba do Sul, RJ. Rev. Bras. Geofísica 27 (2), 225—239.

Officer, C.B., 1976. Physical Oceanography of Estuaries and Associated Coastal Waters. Wiley, London, p. 546.

Schettini, C.A.F., Miranda, L.B., 2010. Circulation and suspended particulate matter in a tidally dominated estuary: Caravelas estuary, Bahia, Brazil. Braz. J. Oceanogr. 58 (1), 1—11.

Schlunz, B., Schneider, R.R., 2000. Transport of terrestrial organic carbon to the oceans by rivers: reestimating flux and burial rates. Int. J. Earth Sci. 88, 599—606.

Syvitski, J.P., Vorosmarty, C.J., Kettner, A.J., Green, P., 2005. Impact of humans on the flux of terrestrial sediment to the global coastal ocean. Science 308, 376e380.

Syvitski, J.P.M., Kettner, A., 2011. Sediment flux and the anthropocene. Philos. Trans. R. Soc. A 369, 957—975.

Valle-Levinson, A., 2010. Conteporary Issues in Estuarine Physics. Cambridge University Press, Cambridge, p. 315.

Weber, M., de Beer, D., Lott, C., Polerecky, L., Kohls, K., Abed, R.M., Ferdelman, T.G., Fabricius, K.E., 2012. Mechanisms of damage to corals exposed to sedimentation. Proc. Natl. Acad. Sci. 109. E1558eE1567.

Weber, M., Lott, C., Fabricius, K., 2006. Sedimentation stress in a scleractinian coral exposed to terrestrial and marine sediments with contrasting physical, organic and geochemical properties. J. Exp. Mar. Biol. Ecol. 336, 18e32.